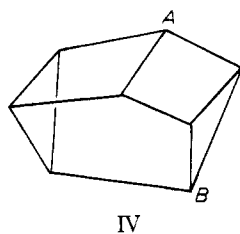


formally distributed in several ways. Generating the same molecular descriptor for resonance structures may be quite advantageous for some applications as documentation. Regarding all resonance structures of a compound as different entities is highly impracticable, if one takes into account the large number of resonance structures which can be drawn for even fairly small molecules. On the other hand, the algorithms described are designed in a way that electronic information like the number of valence electrons of each atom can be handled by including it in the initial labels. This may be necessary, if molecular descriptors for charged species are to be generated. There is in fact no restriction on what kind of initial labels is used, as long as the same kind of atom is associated with the same label, and the order relation \leq is the same for all molecules for which a name is generated.

The reported algorithm works for all chemical structures usually encountered in chemical synthesis. Because of the nature of the atomic descriptors defined there are some exceptional structures in which the maximal numbers of sets of constitutionally equivalent atoms are not found. In the following example atoms A and B are recognized as constitu-



tionally equivalent. They are, however, not equivalent. If such structures are encountered some additional conditions, like the number of ring closures at a certain distance from a vertex,

have to be considered to distinguish the vertices. In order to keep the algorithm as fast as possible this feature has not been included.

The algorithms have been implemented in FORTRAN IV and PL/I and have been extensively used in our synthesis planning program. The fact that constitutional symmetry can be detected leads to a substantial reduction of the number of precursors in the reaction network because generating duplicate precursors can be avoided. The number of precursors is further reduced by the fact that mesomeric structures always get the same descriptor. No precursor is regarded as a different compound merely because the electrons are formally distributed in some other way.

Acknowledgment. We gratefully acknowledge the support of this work by the EC.

References and Notes

- (1) (a) H. J. Hiz, *J. Chem. Doc.*, **4**, 173-180 (1964); (b) L. Spialter, *J. Am. Chem. Soc.*, **85**, 2012-2013 (1963); (c) L. Spialter, *J. Chem. Doc.*, **4**, 261-268 (1964); (d) *ibid.*, **4**, 269-273 (1964); (e) E. Meyer, *Angew. Chem.*, **82**, 605-611 (1970).
- (2) (a) I. Ugi, J. Gasteiger, J. Brandt, J. F. Brunnert, and W. Schubert, *IBM Nachr.*, **24**, 185-189 (1974); (b) I. Ugi, *ibid.*, **24**, 180-184 (1974); (c) J. Brandt, J. Friedrich, J. Gasteiger, C. Jochum, W. Schubert, and I. Ugi, Proceedings of the American Chemical Society Centennial Meeting, New York, N.Y., 1976; (d) J. Brandt, J. Friedrich, J. Gasteiger, C. Jochum, W. Schubert, and I. Ugi, Proceedings of the III International Conference on Computers in Chemical Research, Education, and Technology, Caracas, Venezuela, 1976.
- (3) (a) H. L. Morgan, *J. Chem. Doc.*, **5**, 107-113 (1965); (b) R. H. Penny, *ibid.*, **5**, 113-117 (1965); (c) M. Randic, *J. Chem. Inf. Comput. Sci.*, **15**, 105-108 (1975); (d) W. T. Wipke and T. M. Dyott, *J. Am. Chem. Soc.*, **96**, 4825-4833 (1974).
- (4) C. Jochum and J. Gasteiger, *J. Chem. Inf. Comput. Sci.*, **17**, 113 (1977).
- (5) (a) F. Harary, "Graph Theory", Addison-Wesley, Reading, Mass., 1972, pp 161-163; (b) W. Wagner, "Graphentheorie", B. I. Wissenschaftsverlag, Mannheim, Germany, 1970, pp 100-105.
- (6) J. Blair, J. Gasteiger, C. Gillespie, P. D. Gillespie, and I. Ugi, *Tetrahedron*, **30**, 1845-1859 (1974).

Optimized Geometries of the Saddle-Point Rotamers of Formamide

Roman F. Nalewajski¹

Contribution from the Department of Chemistry, University of North Carolina, Chapel Hill, North Carolina 27514. Received March 22, 1977

Abstract: The ab initio 4-31G fully optimized geometries of the saddle-point rotamers of formamide are reported, with the NH₂ group twisted around the CN bond by 90 and 270°, respectively. The effects of geometry relaxation are discussed in terms of geometry distortions as well as changes in the energy components, dipole moment, and the net charges on atoms. The most important relaxational coordinates were found to be the CN bond length (increase by about 0.05 Å) and the HNH angle (increase by about 13 and 18°, respectively). The predicted variations of these geometrical parameters appear to be consistent with the main change in the electronic structure accompanying the rotation, namely, a lack of delocalization of the nitrogen lone pair into the CO π system in both orthogonal conformers. The energy drops obtained due to geometry optimization (5.64 and 6.24 kcal/mol, respectively) suggest that the rigid-rotation assumption was much responsible for overestimation of the previously reported 4-31G rotational barrier in formamide. Comparisons are made between the ab initio and MINDO geometry relaxational effects, in order to check the validity of the semiempirical SCF MO predictions. The MINDO method was found to fail to predict correctly the lone pair effects in bonded interactions.

Introduction

The investigation of the geometry distortions accompanying inversion and internal rotation in molecular systems is of growing significance in quantum chemistry.² Geometry optimization is essential for reliable assignment of the equilibrium conformers³⁻⁵ and has a considerable effect on the predicted barriers and their components, e.g., ref 4 and 5. In recent years

a number of efficient gradient-type procedures have been developed and applied both within ab initio and semiempirical methods.^{8,9} Energy gradients are directly provided by the ZDO-type semiempirical methods. In ab initio calculations they must be obtained by a finite difference technique, but the effort is also being made to develop methods for direct calculation of energy gradients.¹⁰ The literature^{2,11} already contains many successful applications of the ab initio calculations for

Table I. Geometry Optimization Parameters of the Saddle-Point Rotamers of Formamide

Conformer	$\frac{1}{2} \angle \text{HNH}$	β $\angle \text{HNC}$	γ $\angle \text{HCN}$	δ $\angle \text{NCO}$	a $R(\text{NH})$	b $R(\text{CO})$	c $R(\text{CH})$	d $R(\text{CN})$	Energy, au
$\varphi = 90^\circ$ (Figure 1a)									
Initial geometry	59.7	120.0	113.2	123.8	1.010	1.193	1.102	1.376	-168.640 55
Optimized geometry (4-31G)	66.0	114.7	113.5	125.1	1.000	1.196 ^c	1.077	1.416	-168.649 54
Optimized geometry (MINDO) ^b	50.5	111.6	111.4	122.2	1.147	1.231	1.232	1.439	
Step sizes (Δ , deg, Å)	5.0	10.0	5.0	2.0	0.050		0.050	0.050	
$\varphi = 270^\circ$ (Figure 1b)									
Initial geometry	59.7	120.0	113.2	123.8	1.010	1.193	1.102	1.376	-168.634 69
Optimized geometry (4-31G)	68.7	115.8	117.9	121.4	0.998	1.196	1.084	1.412	-168.644 64
Optimized geometry (MINDO) ^b	38.1	116.5	117.6	119.7	1.162	1.227	1.249	1.435	
Step sizes (Δ , deg, Å)	10.0	10.0	5.0	2.0	0.050	0.020	0.050	0.050	

^a Bond lengths in Å and bond angles in degrees. ^b Reference 5. ^c The optimum value for $\varphi = 270^\circ$ rotamer, not reoptimized for the $\varphi = 90^\circ$ conformer.

Table II. The Energy Gradient, ^a g , and Hessian Matrix, ^b H , for the $\varphi = 90^\circ$ Rotamer of Formamide

	g	H						
		α	β	γ	δ	a	c	d
α	-0.065 ^c	0.202 ^d	-0.120 ^d		0.000 ^d	0.097 ^e		0.002 ^e
β	0.082 ^c		0.332 ^d		-0.007 ^d	-0.053 ^e		0.066 ^e
γ	-0.012 ^c			0.179 ^d	0.097 ^d		-0.002 ^e	0.065 ^e
δ	-0.021 ^c				0.287 ^d		-0.022 ^e	0.063 ^e
a	0.005					1.724		0.000
c	0.028						0.594	0.026
d	0.064							0.918

^a In hartree Å⁻¹ units, if not stated otherwise. ^b Except as noted, units are hartree Å⁻². ^c Units are hartree rad⁻¹. ^d Units are hartree rad⁻². ^e Units are hartree rad⁻¹ Å⁻¹.

determination of equilibrium geometries. It was shown by Freed¹⁴ that effects of geometry relaxation should be correctly represented within Hartree-Fock approximation, since the energy gradient for distortion is the expectation value of a one-electron operator, and by virtue of the extended Brillouin theorem electron correlation does not contribute in first order to the shape of a potential energy surface. Thus, this suggests the use of ab initio geometry optimization as a reliable method for testing the credibility of the semiempirical methods in predicting geometry distortions during internal rotation.

The structure of formamide has been examined extensively both experimentally (by the microwave,^{15a,b} IR,^{15c} and NMR^{15d} spectroscopy, and by x-ray diffraction^{15e}) and theoretically (by ab initio^{12,13,16-18} and semiempirical⁵ molecular orbital calculations). The equilibrium gas-phase structure^{15a,b} (pyramidal model, see Figure 2b) is very satisfactorily reproduced by the MINDO fully optimized geometry.⁵ The fully optimized formamide geometry, obtained using the minimal STO-3G basis set,^{19a} is also in rather satisfactory agreement with experimental data. The formamide rotational barrier,¹² predicted from the frozen-frame ab initio calculations based on the double- ζ 4-31G^{19b} basis set (24.7 kcal/mol), seems somewhat too high compared to the experimental NMR values,²⁰ ranging from 16.8 to 21.3 kcal/mol. In recent years a number of ab initio calculations have been also carried out to investigate the acidic and basic hydrolysis of formamide.^{21,25}

The present ab initio calculations have been carried out in order to determine the complete relaxation effects, accompanying the crossing of the two, $\varphi = 90^\circ$ and $\varphi = 270^\circ$ (φ denotes angle of rotation) barriers. It is also our purpose to confront these variations with the corresponding semiempirical force field results reported in a previous paper,⁵ in order to verify the validity of the MINDO geometry optimized approximation, which is of more general interest in theoretical conformational analysis.

Method

Standard ab initio LCAO MO SCF molecular orbital theory²² has been used. Wave functions and energies for var-

ious geometries of formamide were calculated using the Gaussian 70 program²³ and the split-valence 4-31G basis set,^{19b} which was found to be adequate for both the geometry and energy comparisons. Atomic orbitals were scaled using standard molecular scale factors. For both saddle-point geometries the C_s symmetry has been assumed. Geometry optimization has been performed using Payne's version of the conjugate gradient algorithm,⁹ in which the Hessian matrix H ($H_{ij} = \frac{1}{2}[\partial^2 E/\partial q_i \partial q_j]$) is directly evaluated without recourse to the repeated calculations of the energy gradient $g(Q)$; $Q = [q_1, q_2, \dots, q_N]$ collects the molecular geometrical parameters, defining the starting point on the energy surface $E(Q)$.

The MINDO/2 force field results, compared here with the corresponding ab initio predictions, were taken from ref 5; they have been obtained using the standard set of MINDO parameters reported by Dewar and Lo,²⁴ based on Oleari's method for determining the one-center integrals.

Results

When optimizing the relaxational degrees of freedom of both the $\varphi = 90^\circ$ and $\varphi = 270^\circ$ rotamers of formamide, we have neglected some couplings between geometrical parameters, which are expected to be relatively unimportant. Figures 1a and 1b show the geometrical parameters optimized and the couplings considered. The initial geometries and step sizes Δ_i 's assumed are shown in Table I. The starting geometries are essentially the geometries obtained by corresponding rigid rotations of the NH₂ group in the microwave structure, with small additional adjustments of the $R(\text{NH})$ bond lengths and the CNH bond angles, required by the assumed C_s symmetry constraint.

The calculated gradient (g) and the Hessian matrix (H) for the $\varphi = 90^\circ$ and $\varphi = 270^\circ$ conformers are shown in Tables II and III, respectively. The final minimum energies and the flexible-geometry parameters for both saddle-point rotamers are summarized in Table I and compared with the corresponding values obtained from the MINDO force field calculations. The variations of structural parameters, which accompany the rotation, as determined by ab initio 4-31G cal-

Table III. The Energy Gradient,^a g , and Hessian Matrix,^b H , for the $\varphi = 270^\circ$ Rotamer of Formamide

	g	H							
		α	β	γ	δ	a	b	c	d
α	-0.077 ^c	0.196 ^d	-0.120 ^d	0.001 ^d		0.089 ^e		0.002 ^e	0.001 ^e
β	0.080 ^c		0.332 ^d	0.002 ^d		-0.053 ^e		0.007 ^e	0.063 ^e
γ	-0.027 ^c			0.191 ^d	0.098 ^d	0.000 ^e		0.000 ^e	0.060 ^e
δ	-0.000 ^c				0.275 ^d			-0.032 ^e	0.080 ^e
a	0.007					1.722		0.002	-0.002
b	-0.014						2.125		
c	0.016							0.580	0.034
d	-0.059								0.906

^{a-e} See the corresponding footnotes in Table II.

Table IV. Contributions (in au) to the Total Energies of the Relaxed- and Rigid-Frame Rotamers of Formamide

Energy component	$\varphi = 90^\circ$		$\varphi = 270^\circ$	
	Relaxed geometry	Rigid geometry	Relaxed geometry	Rigid geometry
Nuclear repulsion energy	70.878 83	71.517 98	70.911 49	71.251 54
Total electronic energy	-239.528 37	-240.158 53	-239.556 13	-239.886 23
Electronic kinetic energy	168.755 92	168.796 24	168.743 43	168.768 99
Nuclear-electronic attraction energy	-539.007 85	-540.288 78	-539.127 57	-539.715 65
Electron-electron repulsion energy	130.723 56	131.334 01	130.828 01	131.060 42
Virial ratio ($-V/2T$)	0.999 69	0.999 54	0.999 71	0.999 60

Table V. Comparison of the ab Initio and MINDO^a Dipole Moments (+ \rightarrow -, D) of the Formamide Rotamers^b

φ	Geometry ^c	Method	$-\mu_{\sigma_x}$	μ_y	μ_z	μ_{total}
90°	Relaxed	4-31G	1.909	0.872	0.000	2.098
		MINDO	1.856	0.022	0.000	1.856
	Rigid	4-31G	2.072	0.673	0.000	2.179
		MINDO ^c	2.771	2.074	0.107	3.463
270°	Relaxed	[11,7,1] ^{c,d}	2.227	1.860	0.047	3.949
		4-31G	1.754	3.909	0.000	4.284
		MINDO	1.493	7.136	0.000	7.290
	Rigid	4-31G	2.002	4.193	0.000	4.646
		MINDO ^c	2.732	4.278	-0.110	5.077

^a Reference 5. ^b For the definition of the coordinate system see Figure 1. ^c Rigid structural parameters of the microwave structure.^{15a} ^d Results of the ab initio calculations¹⁸ using the contracted Gaussian basis set including 11 s-type functions, 21 p-type functions (7 p_x , 7 p_y , and 7 p_z), and 6 d-type functions (d_{x^2} , d_{xy} , d_{xz} , d_{yz} , d_{y^2} , d_{z^2}), centered on each heavy atom, and 5 s-type and 3 p-type functions (p_x , p_y , p_z) on each hydrogen atom. ^e The C_s symmetry, if not stated otherwise.

culations, are visualized in Figure 2a, where the microwave values were assumed as reference levels. The analogous MINDO force field diagram is also shown (Figure 2b) for comparison. In Table IV the effect of geometry optimization on various contributions to the total electronic energy is analyzed. The comparisons of the net charges of atoms and dipole moments are presented in Figure 3 and Table V, respectively, both for the ab initio 4-31G and MINDO force field calculations.

Discussion

Geometry Relaxation Effects at the 4-31G Level. Inspection of Tables II and III shows that there are relatively strong α - β , α - α , and γ - δ couplings, in both geometries optimized. It can also be seen that force constants for angles are relatively small, so even large variations of angles due to geometry optimization lead to rather small improvements of the total energies. The actual values of the energy drops for the $\varphi = 90^\circ$ and $\varphi = 270^\circ$ conformers, 0.008 99 (5.64 kcal/mol) and 0.009 95 au (6.24 kcal/mol), respectively, while representing negligible percentages of the total energies, should improve the agreement with experiment of the overestimated 4-31G rigid-rotation barrier in formamide,¹² 24.7 kcal/mol. The reason for this expectation is that the assumption of a near planar, microwave geometry is probably a much better approximation for the $\varphi = 0^\circ$ (equilibrium) conformation than for the perpendicular

$\varphi = 90^\circ$ and $\varphi = 270^\circ$ forms optimized here. Therefore, one should expect a much smaller drop due to optimization of the equilibrium structure than drops obtained for the saddle-point rotamers. As a result, the predicted heights of the flexible-geometry barriers in formamide are expected to be lower than the corresponding rigid-rotation values, thus improving the agreement with experiment.

It follows from the comparison of the energy components collected in Table IV that in both cases the lowering of the total energy due to geometry relaxation is caused by a dominant decrease of the nuclear repulsion component rather than the decrease of the total electronic energy. One can observe also that the increase of the latter contribution results from a controlling increase in the nuclear-electron attraction energy. Note also that values of the virial $-V/2T$ ratio have been slightly improved after geometry optimization.

Returning to the total energies listed in Table I, the difference between barrier heights at the $\varphi = 270^\circ$ and $\varphi = 90^\circ$ positions is predicted to be slightly smaller within the flexible-geometry approximation, 0.004 90 au (3.07 kcal/mol), compared to that resulting from the rigid rotation model, 0.005 86 au (3.68 kcal/mol). This difference might be thought of as being primarily due to the stabilizing attraction between the hydrogen atoms of the NH_2 group (net charges = +0.36) and oxygen atom (net charge = -0.49) (in the $\varphi = 90^\circ$ conformer, Figure 1a), and the destabilizing repulsion between

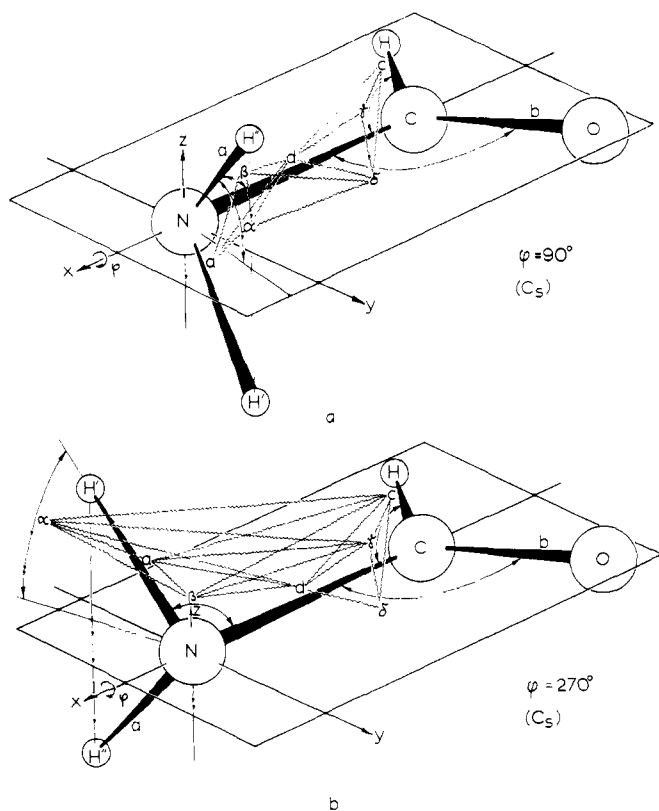


Figure 1. The definitions of the coordinate system, geometrical parameters optimized, and the couplings considered, for the saddle point $\varphi = 90^\circ$ (a) and $\varphi = 270^\circ$ (b) rotamers of formamide. In both cases the C_s symmetry has been assumed.

hydrogen atoms of the NH_2 group (net charges = +0.35) and the hydrogen atom of the CHO group (net charge = +0.16) (in the $\varphi = 270^\circ$ conformer, Figure 1b).

It should be noted finally that in order to obtain quantitative agreement between the calculated and experimental values of rotational barriers in formamide, one should consider the change in the correlation energy during rotation, in addition to geometry relaxation. After rotation of the NH_2 group by $\varphi = 90^\circ$ or $\varphi = 270^\circ$ an increase in the correlation energy in the π bond might be expected. It follows from the generalized valence bond calculations on formamide by Harding and Goddard²⁶ that accounting for this effect alone lowers the predicted barrier height by approximately 4 kcal/mol.

The main variations of the formamide bond lengths (see Table I and Figure 2a), accompanying the rotation of the NH_2 group, are lengthening of the CN bond ($\sim 0.05 \text{ \AA}$) and shortening of the CH bond ($\sim 0.02 \text{ \AA}$). Note that the CO bond length remains approximately constant during rotation. With regard to the angle variations the 4-31G calculations predict a rather large ($\sim 13^\circ$ for $\varphi = 90^\circ$ and $\sim 18^\circ$ for $\varphi = 270^\circ$) increase in the $\text{H}'\text{N}\text{H}''$ bond angle, a decrease in the CNH' and CNH'' bond angles, as well as the increase in the HCN bond angle ($\sim 5^\circ$, only in the $\varphi = 270^\circ$ position). All these changes appear to be consistent with the observed changes in the electronic structure. The CN bond lengthening in the perpendicular rotamers is due to loss of a partly double bond character. The increase in the $\text{H}'\text{N}\text{H}''$ angle of the perpendicular forms is due to repulsion between the N-H bond electron pairs and the lone electron pair on nitrogen, which is not allowed to delocalize over the molecule. Similarly, the increase in the HCN angle for the $\varphi = 270^\circ$ conformer can be interpreted as being caused by the repulsion between the H, H', and H'' hydrogen atoms.

Again, the observed differences between the geometry

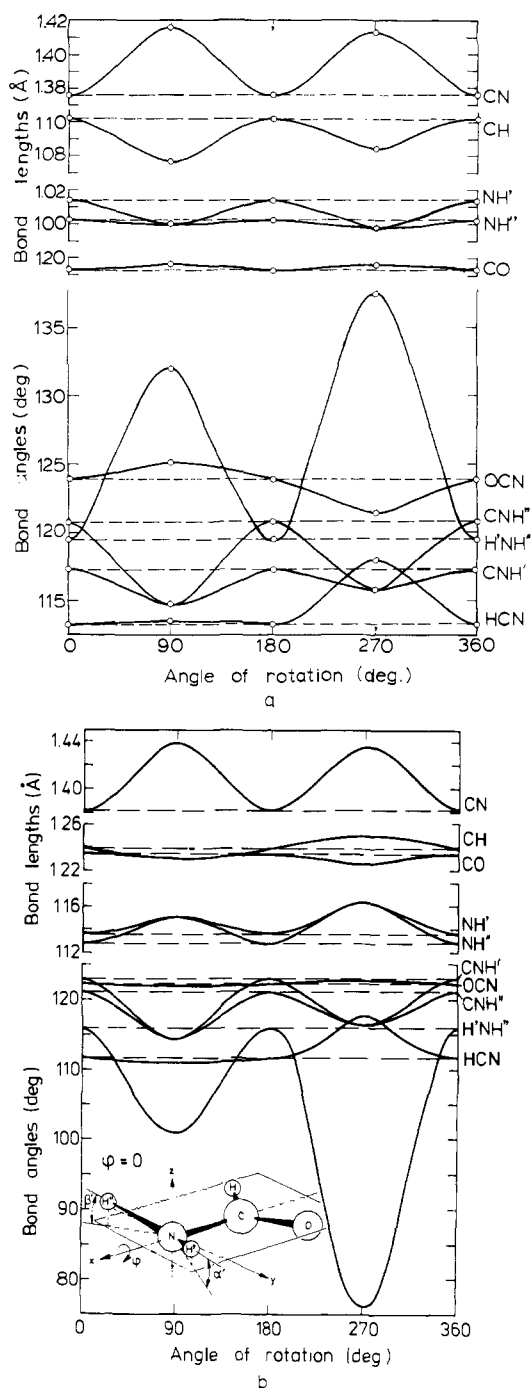


Figure 2. Variations of geometrical parameters of formamide with angle of rotation, as determined by ab initio (a) and MINDO (b) calculations. In the case of ab initio calculations the microwave^{15a} values of structural parameters have been assumed for the $\varphi = 0^\circ$ conformer (not optimized here), with $\alpha' = 6.123^\circ$ and $\beta' = 10.31^\circ$; the corresponding values for the $\varphi = 0^\circ$ MINDO geometrically optimized conformer are $\alpha' = 6.14^\circ$, $\beta' = 10.13^\circ$. Figure 2b is redrawn from ref 5.

variations for the $\varphi = 90^\circ$ and $\varphi = 270^\circ$ rotamers, respectively, might be interpreted in terms of the attraction between the O, H', H'' atoms in the $\varphi = 90^\circ$ form and the repulsion between the H, H', and H'' atoms in the $\varphi = 270^\circ$ form. These effects are the reasons for the differences in the optimum values of the $\text{H}'\text{N}\text{H}''$, HCN, and CNH bond angles. Notice, however, that some trends observed in Figure 2a are inconsistent with such interpretation, e.g., a behavior of the OCN angle. These inconsistencies are probably due to the experimental values of geometrical parameters, assumed as the reference levels.

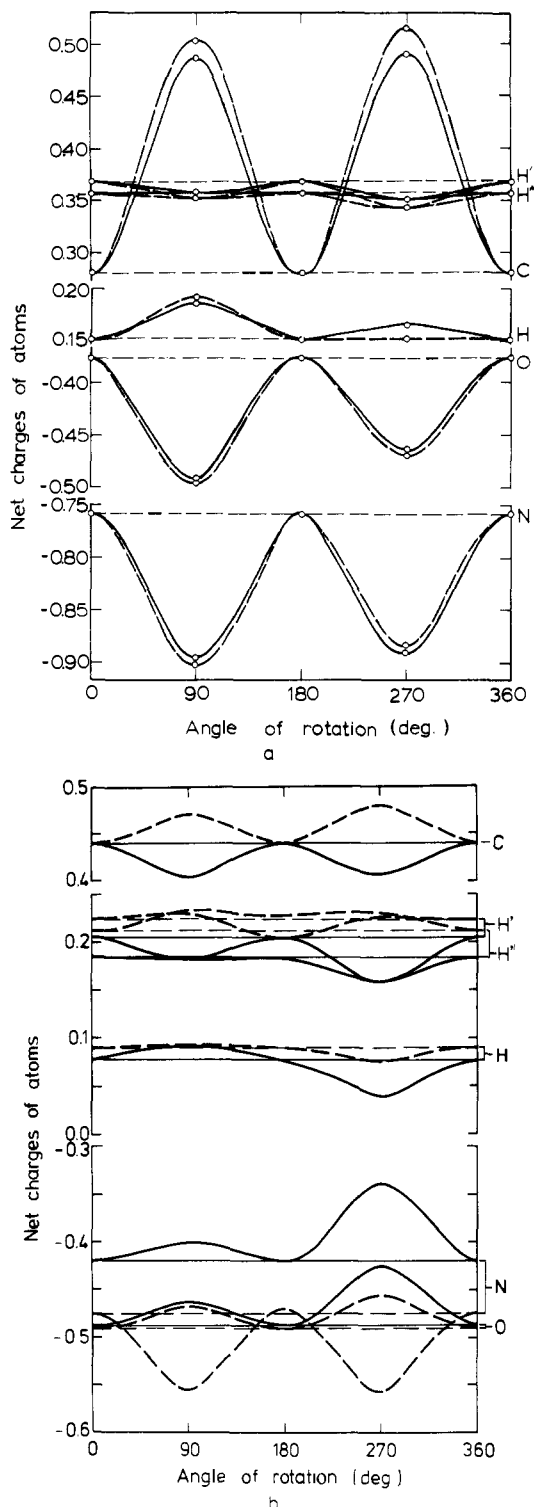


Figure 3. Net charges of atoms in formamide as functions of rotation angle, as determined by ab initio (a) and MINDO (b) calculations. The charges for the $\varphi = 0^\circ$ rotamer in Figure 3a are those reported in ref 16 for the case of the Costain-Dowling geometry,^{15a} obtained using a double ζ contracted Gaussian basis set. Figure 3b is redrawn from ref 5. The solid line curves refer to the optimized geometries while the broken line curves refer to the rigid geometry approximation.

It follows from Figure 3a that geometry optimization introduces rather small correction to the net charges on atoms, resulting from the rigid rotation calculations. The flexible-geometry charges on atoms are slightly diminished, thus leading to a small decrease of the total dipole moments (Table V), compared to those obtained within the rigid-rotation approximation.

Comparison with the MINDO Trends. The most important difference between the predicted 4-31G geometry variations in formamide and those resulting from the MINDO force field calculations (see Table I and Figure 2) can be observed in behavior of the $H'NH''$ angle. In contrast to the ab initio trend the MINDO approximation leads to a rather large decrease in this angle for both saddle-point, orthogonal conformations. As mentioned before, the main factor responsible for variations of this relaxational coordinate is that the delocalization of the nitrogen lone pair into the π system of the CHO group is no longer possible in the orthogonal rotamers. Thus the anisotropy in the electron charge distribution on nitrogen, due to the lone pair contribution, is expected to be essential for the $N-H'$ and $N-H''$ bonded interactions. Within the MINDO (INDO, CNDO) theory, however, the lone pair effects in the interatomic interactions are not represented correctly. The core-core repulsion is represented by spherically symmetric, effective potential, in which the orbital structure is completely disregarded. We expect this to be a reason why the MINDO force field calculations do such a poor job on this type of interaction. It is interesting to note that one should expect much better predictions using the NDDO model, in which the Coulombic part of the two-center interactions is explicitly considered.

The foregoing discussion is consistent with the observed parallel between the ab initio and MINDO, HCN, CNH', and CNH'' curves, shapes of which were found to be primarily determined by the central-field type, $H''-O$, $H'-O$, $H'-H$, and $H''-H$ nonbonded interactions. This suggests that the MINDO (INDO) approximation appears to be reliable in investigating the geometry variations due to nonbonded interactions in molecular systems.

It was shown recently by Gelin and Karplus²⁷ that nonbonded interactions, which are particularly important in the case of steric crowding, can be efficiently estimated within the flexible-geometry empirical potential method.²⁸ They obtained striking parallel between empirical and INDO energies as functions of dihedral angles in β -methylacetylcholine.

We find that the MINDO geometry optimized trends of the net charges on atoms are in sharp contrast to those predicted by the 4-31G ab initio calculations. As a result of the observed differences in charge distribution and geometrical parameters (Table I), the MINDO geometry optimized dipole moments (Table V) differ much from those resulting from the flexible-geometry 4-31G calculations, especially for the $\varphi = 270^\circ$ conformer.

Acknowledgment. This work was supported by the research grant to the University of North Carolina from the National Institutes of Health. The author wishes to thank Professor Robert G. Parr for his constant interest and encouragement, and Dr. Philip W. Payne for helpful conversations.

References and Notes

- (1) Department of Theoretical Chemistry, Jagiellonian University, Krupnicza 41,30-060, Kraków, Poland.
- (2) For a recent review article on the adequacy of the SCF MO treatments of the conformational barriers see P. W. Payne and L. C. Allen, "Theoretical Chemistry", Vol. 4, H. F. Schaefer, Ed., Plenum Press, New York, N.Y., 1976.
- (3) (a) A. Pullman and G. N. J. Port, *Theor. Chim. Acta*, **32**, 77 (1973); (b) G. N. J. Port and A. Pullman, *J. Am. Chem. Soc.*, **95**, 4059 (1973); (c) D. W. Genson and R. E. Christoffersen, *ibid.*, **95**, 362 (1973); (d) R. E. Christoffersen, D. Spangler, G. G. Hall, and G. M. Maggiora, *ibid.*, **95**, 8526 (1973).
- (4) (a) J. C. Rayez and J. J. Dannenberg, *Chem. Phys. Lett.*, **41**, 492 (1976); (b) J. Pancir, *Theor. Chim. Acta*, **40**, 81 (1975).
- (5) R. F. Nalewajski, *Z. Naturforsch. A*, **32**, 276 (1977).
- (6) (a) R. Fletcher and M. J. D. Powell, *Comput. J.*, **6**, 163 (1963); (b) M. J. D. Powell, *ibid.*, **7**, 155 (1964); (c) R. Fletcher, *ibid.*, **13**, 317 (1970); (d) B. A. Murtagh and R. W. H. Sargent, *ibid.*, **13**, 185 (1970); (e) for a recent review article on these optimization techniques see D. Garton and B. T. Sutcliffe, "Theoretical Chemistry", Vol. 1, R. N. Dixon, Ed., Specialist Reports of the Chemical Society, Chemical Society, London, 1974, p 34.
- (7) (a) J. W. McIver and A. Komornicki, *Chem. Phys. Lett.*, **10**, 303 (1971); J.

- Am. Chem. Soc.*, **94**, 2625 (1972); **95**, 4512 (1973); (b) P. Pulay and F. Török, *Mol. Phys.*, **25**, 153 (1973); (c) J. Pančič, *Theor. Chim. Acta*, **29**, 21 (1973); *Collect. Czech. Chem. Commun.*, **40**, 1112, 2726 (1975); (d) R. C. Bingham, M. J. S. Dewar, and D. H. Lo, *J. Am. Chem. Soc.*, **97**, 1285 (1975).
- (8) (a) R. F. Nalewajski and A. Gojebiewski, *Acta Phys. Pol. A*, **49**, 683 (1976); (b) R. F. Nalewajski, *J. Mol. Struct.*, **40**, 247 (1977).
- (9) P. W. Payne, *J. Chem. Phys.*, **65**, 1920 (1976).
- (10) (a) P. Pulay, *Mol. Phys.*, **17**, 197 (1969); **18**, 473 (1970); (b) H. B. Schlegel, S. Wolfe, and F. Bernardi, *J. Chem. Phys.*, **63**, 3632 (1975); (c) A. Gojebiewski, *Mol. Phys.*, **32**, 1529 (1976).
- (11) W. A. Lathan, L. A. Curtiss, W. J. Hehre, J. B. Lisle, and J. A. Pople, *Prog. Phys. Org. Chem.*, **11**, 175 (1974).
- (12) L. Radom, W. A. Lathan, W. J. Hehre, and J. A. Pople, *Aust. J. Chem.*, **25**, 1601 (1972).
- (13) J. P. Daudey, the STO-3G fully optimized geometry reported in ref 21a.
- (14) K. F. Freed, *Chem. Phys. Lett.*, **2**, 255 (1968).
- (15) (a) C. C. Costain and J. M. Dowling, *J. Chem. Phys.*, **27**, 585 (1957); (b) M. Kitano and K. Kuchitsu, *Bull. Chem. Soc. Jpn.*, **47**, 67 (1974); (c) J. C. Evans, *J. Chem. Phys.*, **22**, 1228 (1954); (d) R. A. Kromhout and G. W. Moulton, *ibid.*, **25**, 35 (1956); (e) C. Post and J. Ladell, *Acta Crystallogr.*, **7**, 559 (1954).
- (16) H. Basch, M. B. Robin, and N. A. Kuebler, *J. Chem. Phys.*, **47**, 1201 (1967); **49**, 5007 (1968).
- (17) M. A. Robb and I. G. Csizmadia, *Theor. Chim. Acta*, **10**, 269 (1968); *J. Chem. Phys.*, **50**, 1819 (1969).
- (18) D. Christensen, R. N. Kortzeborn, B. Bak, and J. J. Led, *J. Chem. Phys.*, **53**, 3912 (1970).
- (19) (a) W. J. Hehre, R. F. Stewart, and J. A. Pople, *J. Chem. Phys.*, **51**, 2657 (1969); (b) R. Ditchfield, W. J. Hehre, and J. A. Pople, *ibid.*, **54**, 724 (1971).
- (20) (a) B. Sunners, L. H. Piette, and W. G. Schneider, *Can. J. Chem.*, **38**, 681 (1960); (b) H. Kamei, *Bull. Chem. Soc. Jpn.*, **41**, 2269 (1968).
- (21) (a) A. M. Armbruster and A. Pullman, *FEBS Lett.*, **49**, 18 (1974); (b) A. Pullman, *Chem. Phys. Lett.*, **20**, 29 (1973); (c) A. C. Hopkinson and I. G. Csizmadia, *Can. J. Chem.*, **51**, 1432 (1973); (d) R. Bonaccorsi, A. Pullman, E. Scrocco, and J. Tomasi, *Chem. Phys. Lett.*, **12**, 622 (1972).
- (22) C. C. J. Roothaan, *Rev. Mod. Phys.*, **23**, 69 (1951).
- (23) W. J. Hehre, W. A. Lathan, R. Ditchfield, M. D. Newton, and J. A. Pople, Gaussian 70, Quantum Chemistry Program Exchange, Program 236.
- (24) M. J. S. Dewar and D. H. Lo, *J. Am. Chem. Soc.*, **94**, 5296 (1972).
- (25) G. Alagona, E. Scrocco, and J. Tomasi, *J. Am. Chem. Soc.*, **97**, 6976 (1975).
- (26) L. B. Harding and W. A. Goddard III, *J. Am. Chem. Soc.*, **97**, 6300 (1975).
- (27) B. R. Gelin and M. Karplus, *J. Am. Chem. Soc.*, **97**, 6996 (1975).
- (28) S. Lifson and A. Warshel, *J. Chem. Phys.*, **49**, 5116 (1968); A. Warshel and S. Lifson, *ibid.*, **53**, 582 (1970); A. Warshel, M. Levitt, and S. Lifson, *J. Mol. Spectrosc.*, **33**, 84 (1970); M. Karplus and S. Lifson, *Biopolymers*, **10**, 1973 (1971).

The Conformation of Echinomycin in Solution

H. T. Cheung,^{†1a} J. Feeney,^{*1a} G. C. K. Roberts,^{1a} D. H. Williams,^{1b} G. Ughetto,^{‡1c} and M. J. Waring^{1c}

Contribution from the National Institute for Medical Research, Mill Hill, London, NW7 1AA, England, and the University Chemistry Laboratory and the Pharmacology Department, University of Cambridge, Cambridge, England.
Received May 23, 1977

Abstract: We have investigated the ¹H and ¹³C NMR spectra of echinomycin in deuteriochloroform and dimethyl-*d*₆ sulfoxide solution. From a consideration of the measured NMR parameters and the results of model building and potential energy calculations we have deduced the conformation of echinomycin in solution.

Introduction

Echinomycin is an antibiotic whose biological effects are attributable to an inhibition of DNA template activity.^{2,3} The molecule is a cyclic octapeptide incorporating a thioacetal cross-linkage and two quinoxaline rings^{4,5} (structure I). The binding of echinomycin to DNA has been shown^{6,7} to occur by the simultaneous intercalation of both quinoxaline rings between the base pairs. In order to explore the structural basis of this novel bifunctional intercalative binding, it is necessary to establish the conformational structure of echinomycin. We report here nuclear magnetic resonance data, model-building studies, and semiempirical potential energy calculations which together allow us to describe the conformation of echinomycin in solution.

Experimental Section

Echinomycin (supplied by Ciba-Geigy, Switzerland) was examined at concentrations between 2 mM and 110 mM in deuteriochloroform or deuteriodimethyl sulfoxide, containing hexamethyldisiloxane (HMS) as a chemical shift reference.

The NMR spectra were obtained using Bruker WH 270 (¹H, 270 MHz), Varian SC300 (¹H, 300 MHz), and Varian XL 100 (¹H, 100 MHz; ¹³C, 25.2 MHz) spectrometers equipped with Fourier transform facilities. All measurements were made in the Fourier transform mode of operation using acquisition times of up to 4 s. When the highest resolution was required, spectral widths of 3 kHz were digitized over 12K words.

[†] Pharmacy Department, University of Sydney, Sydney, Australia.

[‡] Laboratorio di Strutturistica Chimica Giordano Giacomello, Montelibretti, Rome, Italy.

La(fod)₃ and Eu(fod)₃ (fod = 1,1,1,2,2,3,3-heptafluoro-7,7-dimethyl-4,6-octanedionate) were obtained from Digby Chemical Services, London. Aliquots of a concentrated (~25 mM) solution of La(fod)₃ or Eu(fod)₃ were added to solutions of echinomycin in deuteriochloroform (19 and 9 mM, respectively).

Details of the procedures used for the semiempirical potential energy calculations have been given elsewhere.⁸

Results and Discussion

The thioacetal cross-linkage in echinomycin introduces an asymmetry into the molecule causing the two halves to be nonequivalent. This nonequivalence is manifested in both the ¹H and ¹³C NMR spectra where multiplets with different chemical shifts are observed for some of the nuclei occupying corresponding positions in the two halves of the molecule. Thus in the ¹H NMR spectrum of echinomycin in CDCl₃ at 270 MHz (Figures 1 and 2) we see two different absorptions for the D-Ser NH, Ala NH, Ala CH₃, NCH₃ of NMe Val and NMe Cys, and the Val CH₃ nuclei.

A partial assignment of the ¹H spectrum at 100 MHz has already been reported;⁵ the remaining assignments were made by spin decoupling experiments at 270 and 300 MHz.

¹H Chemical Shifts. The ¹H chemical shifts for echinomycin in CDCl₃ and Me₂SO-*d*₆ were measured at different temperatures and the results are summarized in Table I. Most of the nuclei have shifts similar to those observed in simple dipeptides; however, the D-Ser NH and the CysαCH resonances are considerably to low field of where they normally absorb. The low-field shift of the D-Ser NH is easy to explain in terms of ring current shifts from the quinoxaline rings attached to